Temporal Effect of Functional Blocking of β 1 Integrin on Cell Adhesion Strength under Serum Depletion

ARTICLE *in* LANGMUIR · OCTOBER 2009

Impact Factor: 4.46 · DOI: 10.1021/la901527x · Source: PubMed

5 AUTHORS, INCLUDING:

Ning Cai
Wuhan Institute of Technology
26 PUBLICATIONS **133** CITATIONS

SEE PROFILE

Langmuir Article

pubs.acs.org/Langmuir

Temporal Effect of Functional Blocking of β_1 Integrin on Cell Adhesion Strength under Serum Depletion

Ning Cai, Chee C. Wong, Samuel C. W. Tan, Vincent Chan, and Kin Liao*

School of Chemical and Biomedical Engineering, Nanyang Technological University, Singapore 639798

Received April 29, 2009. Revised Manuscript Received June 15, 2009

Cell adhesion is generally concomitant to the formation of focal adhesion. Although it is well-known that focal adhesion plays an important role in the functional regulations of anchorage dependent cells, previous experimental studies have not provided quantitative description of the relation between focal adhesion and biophysical responses of cells. Furthermore, there is lack of knowledge on the importance of the β_1 integrin subunit to the dynamic responses of cells during initial cell seeding. In this study, we attempt to bridge the quantitative connection between focal adhesion density and cell-substrate interactions and evaluate the influence on functional blocking of β_1 integrin on adhesion strength. Total internal reflection fluorescence microscopy (TIRFM), fluorescence microscopy, and phase contrast microscopy was employed to study the time-dependent evolvement of vinculin pattern, distribution of actin filament, and morphological change, respectively, during 4 h of culture for porcine esophageal fibroblasts (non-blocked and β_1-blocked) on a fibronectin-coated surface. Micropipet aspiration technique was used to study the change of mechanotransduction through the determination of adhesion force and strength. It is shown in our experimental results that spread area, adhesion force, and adhesion strength increases over time on the two types of cells. Throughout the culture period, the two key mechanotransduction parameters of non-blocked cells is higher than those of β_1-blocked cells. Interestingly, adhesion strength initially ascends, then begins to diminish at a critical time point, and finally resumes increasing linearly against the increase of focal adhesion density. This variation as mentioned above can be explained by peeling and fracture models based on the dissimilar vinculin pattern of cells after being cultured for different time periods. Moreover, the averaged focal adhesion strength and non-focal adhesion strength of β_1-blocked cells are significantly less than those of non-blocked of cells. The weaker adhesion strength on β_1-blocked cells is directly caused by lower focal and non-focal adhesion strength, as well as by smaller focal adhesion density.

1. Introduction

Cell adhesion to extracellular matrix (ECM) is critical to many physiological processes such as cell migration, tissue organization, and cell differentiation.[1] Interactions between cells and ECM are mediated through transmembrane receptors called integrins. Integrin-mediated adhesion is a dynamic process composed of two major stages: the initial ligand-integrin receptor binding and the following adhesion strengthening process which involves a series of post-binding events, including integrin clustering, recruitment of structure proteins to form focal adhesion, and cytoskeleton remodeling.[4,5] Focal adhesions, specific sites on the cell membrane where integrins link ECM to cytoskeleton, contains multiple structural proteins such as vinculin, talin, paxillin, as well as signaling proteins including focal adhesion kinase (FAK).[2,6] Focal adhesions not only mechanically combine with integrins and cytoskeleton, but also act as a signaling hub to relay biochemical and mechanical stimuli from the extracellular environment to cell nucleus.[7,8]

Integrin-mediated adhesion has been extensively studied with the intent to decipher its mechanism.[2,3] However, most of these efforts were focused on seeking the proteins involved in cell adhesion and the downstreaming signal transduction pathway,[3] and less attention has been paid to the mechanical aspect of cell adhesion.[9] For example, although the positive influence of focal adhesion density on overall adhesion strength has been observed previously by researchers,[9,10] there is still a lack of experimental results to quantitatively correlate adhesion strength with focal adhesion density.

Fibronectin is one of key components in ECM which can be recognized by various integrin receptors such as $\alpha_5\beta_1$, $\alpha_{II}\beta_3$, $\alpha_4\beta_1$, and $\alpha_V\beta_3$.[11] Among fibronectin-binding receptors, integrin $\alpha_5\beta_1$ is the primary receptor in mediating integrin-fibronectin interactions.[11] The β_1 integrin subunit plays a key role in $\alpha_5\beta_1$ integrin-mediated adhesion.[12] The cytoplasmic domains of β_1 integrin subunits are indispensable in the establishment of these connections between focal adhesion protein and actin filament.[13] It has been found that altered expression of the β_1 integrin affects both physiological and pathological processes including epidermal growth, neural differentiation development, wound healing, and tumor angiogenesis.[14−17] In contrast to the clear

*To whom correspondence should be addressed. E-mail: askliao@ntu.edu.sg. Phone: (65)6790-5835. Fax: (65)67911761.

(1) Gumbiner, B. M. *Cell* **1996**, *84*, 345–357.
(2) Giancotti, F. G.; Ruoslahti, E. *Science* **1999**, *285*, 1028–1032.
(3) Hynes, R. O. *Cell* **2002**, *110*, 673–687.
(4) Lotz, M. M.; Burdsal, C. A.; Erickson, H. P.; McClay, D. R. *J. Cell Biol.* **1989**, *109*, 1795–1805.
(5) Gallant, N. D.; Garcia, A. J. *J. Biomech.* **2007**, *40*, 1301–1309.
(6) Carragher, N. O.; Frame, M. C. *Trends Cell Biol.* **2004**, *14*, 241–249.
(7) Geiger, B.; Bershadsky, A. *Cell* **2002**, *110*, 139–142.
(8) Geiger, B.; Spatz, J. P.; Bershadsky, A. D. *Nat. Rev. Mol. Cell Biol.* **2009**, *10*, 21–33.
(9) Gallant, N. D.; Michael, K. E.; Garcia, A. J. *Mol. Biol. Cell* **2005**, *16*, 4329–4340.
(10) Griffin, M. A.; Engler, A. J.; Barber, T. A.; Healy, K. E.; Sweeney, H. L.; Discher, D. E. *Biophys. J.* **2004**, *86*, 1209–1222.
(11) Johansson, S.; Svineng, G.; Wennerberg, K.; Armulik, A.; Lohikangas, L. *Front. Biosci.* **1997**, *2*, d126–146.
(12) Al-Jamal, R.; Harrison, D. J. *Pharmacol. Ther.* **2008**, *120*, 81–101.
(13) Bershadsky, A. D.; Balaban, N. Q.; Geiger, B. *Annu. Rev. Cell Dev. Biol.* **2003**, *19*, 677–695.
(14) Andressen, C.; Arnhold, S.; Puschmann, M.; Bloch, W.; Hescheler, J.; Fassler, R.; Addicks, K. *Neurosci. Lett.* **1998**, *251*, 165–168.
(15) Grose, R.; Hutter, C.; Bloch, W.; Thorey, I.; Watt, F. M.; Fassler, R.; Brakebusch, C.; Werner, S. *Development* **2002**, *129*, 2303–2315.
(16) Watt, F. M. *EMBO J.* **2002**, *21*, 3919–3926.
(17) Mettouchi, A.; Meneguzzi, G. *Eur. J. Cell Biol.* **2005**, *85*, 243–247.

understanding of the function of β_1 in other physiological process, the influence of functional blocking of integrin β_1 on adhesion strength and focal adhesion formation is poorly known.

Total internal reflection fluorescence microscopy (TIRFM) is a powerful technique to analyze processes near the cell membrane.[18] This technique allows molecules which are in a layer of around 100 nm above the coverslip to be excited.[19] Using TIRFM, focal adhesion can be examined by visualizing the fluorescently labeled focal adhesion proteins.[20] Particularly, vinculin is often chosen to be stained because of easy availability of commercial antibodies against it and its ubiquitous presence in various types of cells.[21] Because of the unique capability of TIRFM to selectively illuminate only the cell-substrate interface, cytoplasmic vinculin will not produce the interference to TIRFM images of vinculin. With extremely high signal-to-noise ratio, the acquired clear TIRFM images of the focal adhesion complex are fit for quantitative analysis.

Currently, little is known on temporal effect of functional blocking of β_1 integrin on cell adhesion strength. The motivation of this study is to explore the quantitative relation among adhesion strength, focal adhesion density, and cell spreading, as well as the contribution of β_1 integrin subunit to the adhesion strengthening process. In the present work, fibronectin coated surface was used as a model ECM. Adhesion-blocking antibody was employed to inhibit the function of the integrin β_1 subunit in porcine esophageal fibroblasts (PEFs). The evolution of cell morphology, F-actin distribution, and vinculin pattern in non-blocked and β_1-blocked PEFs during 4 h of culture was examined by phase contrast microscopy, fluorescence microscopy, and TIRFM, respectively. Time-dependent change of adhesion force of non-blocked and β_1-blocked PEFs on a fibronectin-coated surface was measured by the micropipet aspiration technique. As serum contains various types of unknown proteins which may enhance cell adhesion, all of our adhesion experiments were carried out in serum free condition, where only coated fibronectin is involved in integrin-mediated adhesion. On the basis of data acquired in our experiments, the contribution of cell spreading and variaion of focal adhesion density to adhesion strengthening process are studied and interpreted, and the effect of functional blocking of integrin β_1 on adhesion strength are discussed.

2. Experimental Section

2.1. Materials. Dulbecco's modified eagle medium (DMEM), penicillin-streptomycin solution, fetal bovine serum (FBS), Trypsin-EDTA, and Alexa Fluor 635 phalloidin were purchased from Invitrogen (U.S.A.). Phosphate buffer saline, fibronectin, QuantiPro bicinchoninic acid (BCA) assay kit, paraformaldehyde, 4′,6-diamidino-2-phenylindole (DAPI), and Triton X-100 were obtained from Sigma-Aldrich Chemical Inc. (U.S.A.). Mouse anti-vinculin monoclonal antibody and FITC conjugated Goat anti-Mouse IgG were provided by Chemicon (U.S.A.).

2.2. Surface Preparation and Characterization. The glass coverslips used in our experiment were first immersed in piranha solution (3:7, H_2SO_4/H_2O_2) solution for 1 h at 80 °C, then rinsed with a great amount of deionized water (18 MΩ), and finally dried in an oven at 100 °C for 1 h. The cleaned coverlips were sterilized through 2 h of UV exposure before protein coating. To prepare fibronectin-coated coverslips, a fibronectin solution (0.6 mg/mL in PBS) was placed onto the surface of each coverslip. After incubation overnight at 4 °C, the coverslips were washed three times with PBS.

Atomic force microscope (AFM, Veeco Inc., U.S.A.) was employed to examine the morphology of the fibronectin-coated surface and the control surface (uncoated coverslip). The AFM images were processed and analyzed using the Nanoscope Software v5.31. (Veeco Inc., U.S.A.).

The sessile drop technique was used for the contact angle measurement by a contact angle measuring apparatus (FTA 1000, First Ten Angstroms Inc., U.S.A.). Water droplets were put on the sample surface, and their images were taken. Water contact angle was obtained by analyzing the image of each droplet. The average value of contact angle was calculated based on 15 data points collected from 3 sample surfaces.

The density of coated fibronectin was quantitated by QuantiPro BCA assay according to the protocol provided by the manufacturer. This measurement was repeated five times to obtain a mean value.

2.3. Cell Culture and Integrin Blocking. Porcine Esophageal fibroblast was isolated from porcine esophagus by a previously published protocol.[22] Cells were grown in DMEM supplemented with 100 U/mL penicillin, 100 U/mL streptomycin, and 10% fetal bovine serum. Cells were subcultured twice a week using trypsin-EDTA and maintained in a humidified incubator at a temperature of 37 °C in 5% CO_2. The passage number of cells used in all experiments ranges from 6 to 10.

Anti-integrin β_1 antibodies were applied to block binding of integrin β_1 to fibronectin. To prepare non-blocked PEFs (the control group) and integrin β_1-blocked PEFs (the experimental group), cells were harvested and suspended in blocking buffer (0.5% BSA in DMEM) to a final density of 1×10^6 cells/mL. Then cells in blocking buffer were maintained at 4 °C for 30 min.

For the control group, cells were kept in this condition for another 30 min. For the experiment group, monoclonal anti-integrin β_1 antibodies (4B4 clone, Beckman Coulter, U.S.A.) were added into cell solution at a volume ratio of 1:100, and the cells were incubated in blocking buffer with antibodies at 4 °C for 30 min. Before usage, non-blocked and β_1-blocked PEFs were collected by centrifugation followed by the dispersion in DMEM.

2.4. Immunostaining of F-actin and Vinculin. Non-blocked and β_1-blocked PEFs were seeded onto fibronectin-coated coverslips. After cultured for different time periods, cells were fixed with 4% paraformaldehyde in PBS for 30 min followed by washing twice with wash buffer (PBS containing 0.05% Tween-20) at room temperature. The cells were then permeabilized with 0.1% Triton X-100 in PBS for 10 min. Following two washes with wash buffer, the sample was saturated with blocking solution (1% BSA in PBS) for 40 min. After an overnight incubation in dark at 4 °C with mouse anti-vinculin monoclonal antibodies (1:300 dilution in blocking solution), the sample was washed three times with wash buffer again. Finally, FITC conjugated Goat anti-Mouse IgG at 1:300 dilution in PBS was applied together with Alexa Fluor 635 phalloidin (3 Unit/mL) to the sample for 1 h at room temperature. The stained sample was covered with antifade mounting solution (Vector laboratories, U.S.A.) for microscopy observation.

2.5. Total Internal Reflection Fluorescence Microscopy. The TIRFM system is based on Zeiss Axiovert inverted microscope system (Carl Zeiss, Germany) equipped with a 100× 1.45NA objective lens (Carl Zeisss, Germany), a 488 nm argon laser, and X-Cite 120 fluorescence illumination system. FITC-labeled vinculin (Green) was detected in TIRFM mode

(18) Schneckenburger, H. *Curr. Opin. Biotechnol.* **2005**, *16*, 13–18.
(19) Gingell, D.; Todd, I.; Bailey, J. *J. Cell Biol.* **1985**, *100*, 1334–1338.
(20) Petit, V.; Thiery, J. P. *Biol. Cell* **2000**, *92*, 477–494.
(21) Owen, G. R.; Meredith, D. O.; ap Gwynn, I.; Richards, R. G. *Eur. Cell. Mater.* **2005**, *9*, 85–96.
(22) Zhu, Y. B.; Chian, K. S.; Chan-Park, M. B.; Mhaisalkar, P. S.; Ratner, B. D. *Biomaterials* **2006**, *27*, 68–78.

with excitation at 488 nm. Alexa Fluor 635-labeled actin (Red) was visualized using an X-cite 120 illumination system. In addition, a bright field image was also taken for the same field of vision to examine cell morphology.

2.6. Cell Adhesion Force and Strength. Cell adhesion force was measured with a micropipet aspiration system. Its complete setup was described in details elsewhere.[23] Before measurement, a coverslip with adherent cells cultured on fibronectin-coated surface for specified time was mounted onto the stage of an inverted microscope. Before measurement, one adherent cell was chosen randomly and a phase contrast image was taken to capture its shape. During measurement, the micropipet was manipulated to aspirate and pull a small portion of the cell, while the real time detachment process was monitored by the CCD camera embedded in the inverted microscope. Initially, a cell cannot be detached from the surface as the aspiration force (calculated by multiplying the aspiration pressure by the cross-sectional area of the micropipet tip) is not big enough. The aspiration and retraction of cell was repeated with the stepwise increases in aspiration pressure until the cells were separated from the surface and moved together with the micropipet. The minimum aspiration force applied to dissociate an adherent cell from the surface is taken as the adhesion force. Correspondingly, adhesion strength is determined by dividing adhesion force by cell spread area, acquired from phase contrast images of adherent cells.

2.7. Analysis of Images. All images were analyzed using using ImageJ (National Institute of Health, U.S.A.) to measure cell spread area and focal adhesion area. Focal adhesion area was acquired by following a published procedure.[24] First, TIRFM image of vinculin was converted into a gray level image. Then the binary image was generated. The threshold was calculated by the formula (Threshold = Mean-SD) where Mean and SD refer to the average value and standard deviation of the gray level distribution of all pixels, respectively. Finally, focal contact area was obtained from the binary image.

2.8. Cell Attachment Assay. Cells were plated onto fibronectin-coated surface at about 5×10^4 cells/cm^2. Following each incubation period, the surfaces were rinsed with PBS to remove unbound cells. The adhered cells were fixed using 4% paraformaldehyde in PBS for 20 min followed by permeabilization in 0.2% Triton X-100 for 2 min. After three washes with PBS, cell nuclei were stained by DAPI (50 ng/mL). For counting cells, at least 20 separate zones on each substrate were imaged at 200 times amplification by an Olympus IX71 microscope. Each assay was repeated five times separately for each type of cells.

2.9. Statistical Analysis. All data is shown as mean ± standard deviation. Statistical analysis was performed by the unpaired Student's t test. A value of $p < 0.05$ was considered statistically significant.

3. Results

3.1. Surface Characterization. The topographic morphology of uncoated coverslip and fibronectin-coated coverslip was examined by AFM. The AFM images of the uncoated coverslip and fibronectin-coated coverslip in phase and height mode are shown in Figure 1. It is displayed in Figure 1, panels A and B, that the uncoated glass surface is rather smooth. Only a few of spherical bulges and dents, possibly brought on by the fabrication process, were found in some parts of the region examined. In contrast, fibronectin lies on a smooth coverslip surface in globular form as shown in Figure 1, panels C and D. Furthermore, the

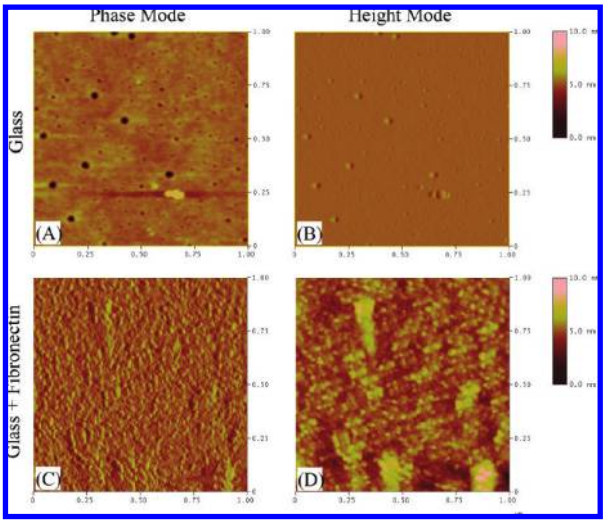

Figure 1. AFM images of uncoated glass coverslip and fibronectin-coated glass coverslip.

root-mean-square (rms) roughness of uncoated coverslip and fibronectin-coated coverslip are 0.31 ± 0.03 nm and 1.13 ± 0.15 nm ($p < 0.05$), respectively. The immobilization of fibronectin on clean coverslip brought the increase of roughness. Similar variation in morphology after fibronectin coating on glass was also seen by other researchers.[25] To determine the hydrophobic/hydrophilic nature of the two surfaces, contact angle measurement was implemented. The contact angle of uncoated coverslip and fibronectin-coated coverslip is 39 ± 2° and 94 ± 3° ($p < 0.01$), respectively, indicating the hydrophilic nature of uncoated coverslip surface was turned significantly more hydrophobic following fibronectin coating. In addition, the density of fibronectin on fibronectin-coated coverslip was quantified to be 0.45 ± 0.06 mg/cm^2 by BCA assay, which is nearly the double of fibronectin monolayer density (0.25 mg/m^2),[26] revealing that more than one layer of fibronectin was deposited onto the coverslip .

3.2. Time-Dependent Cell Spreading and Morphological Change. Cell adhesion is often accompanied by the change in cell morphology.[27] To investigate the adhesion process of non-blocked and β_1 integrin-blocked PEFs on fibronectin-coated, adherent cells were examined by phase contrast microscopy. Phase contrast and immunofluorescence images of F-actin and vinculin for a typical non-blocked PEF on fibronectin-coated surface within 4 h after cell seeding are shown Figure 2. As demonstrated in Figure 2A−F, the non-blocked cell significantly spreads during 4 h of culture. At the same time, the cell is transformed into polygonal morphology from a round shape. The β_1 integrin submit is a major component of fibronectin receptor prototype, $\alpha_5\beta_1$ integrin,[11] and blocking the β_1 subunit affects ligand−receptor interaction, possibly altering the time course of the morphological change. Phase contrast and immunofluorescence images of F-actin and vinculin for a typical β_1-blocked PEF on fibronectin-coated surface within 4 h after cell seeding are shown Figure 3. It is noticed in Figure 3A−F that the β_1-blocked cell on a fibronectin-coated surface also goes through cell spreading and morphological evolution during 4 h of culture, very similar to the non-blocked cell. However,

(23) Tan, S. C. W.; Pan, W. X.; Ma, G.; Cai, N.; Leong, K. W.; Liao, K. *BMC Cell Biol.* **2008**, *9*, 71.
(24) Kim, Y. J.; Park, S.; Lee, Y. J.; Shin, J. W.; Kim, D. H.; Heo, S. J.; Park, K. D. *J. Biomed. Mater. Res. B* **2008**, *85B*, 353–360.
(25) Vallieres, K.; Chevallier, P.; Sarra-Bournett, C.; Turgeon, S.; Laroche, G. *Langmuir* **2007**, *23*, 9745–9751.
(26) Goodman, S. L.; Cooper, S. L.; Albrecht, R. M. *J. Biomed. Mater. Res.* **1993**, *27*, 683–695.
(27) Price, L. S.; Leng, J.; Schwartz, M. A.; Bokoch, G. M. *Mol. Biol. Cell* **1998**, *9*, 1863–1871.

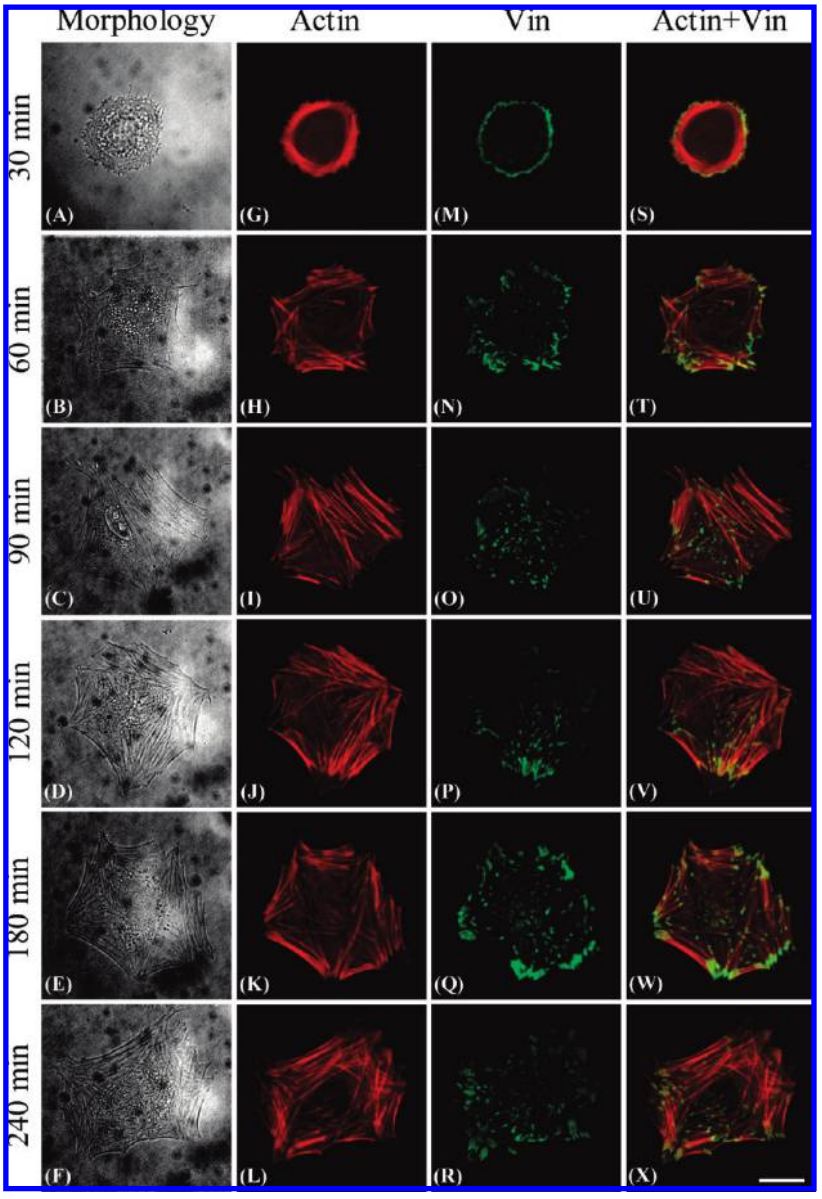

Figure 2. Time course study of cell morpholgy, F-actin distribution, and vinculin pattern of non-blocked PEFs. (A)−(F), phase contrast images; (G)−(L), fluorescence images of F-actin; (M)−(R), fluorescence images of vinculin; S−X, merged images of F-actin and vinculin. Vin = vinculin. Bar, 20 μm.

the initiation of change in cell shape for the β_1-bocked PEF lags behind the non-blocked cell. For the non-blocked cell, it displays polygonal morphology after only 60 min of culture (Figure 2B). In contrast, the β_1-blocked cell maintains a nearly round shape within 90 min (Figure 3A−C). This difference reflects that the β_1 integrin subunit exerts important influence on the cell adhesion process. To quantitatively compare the spreading process of non-blocked and β_1-blocked cells, phase contrast images were analyzed to obtain spread area. Figure 4 shows the plot of spread area against culture time for non-blocked and β_1-blocked PEFs on a fibronectin-coated surface. The result indicates that either non-blocked or β_1-blocked cells keep on spreading after cell seeding. During the initial 90 min of culture, non-blocked cells possess higher spread area than β_1-blocked cells. However, after 240 min of culture, the spread area of the two types of cells is almost comparable. At 240 min, spread area of non-blocked and β_1-blocked cells are 2855 μm^2 and 2712 μm^2 ($P > 0.05$), respectively, indicating there is no significant difference in extent of spread for the two type of cells. The independence of final spreading extent on β_1 integrin blocking also occurs in osteoblasts, chondrocytes, and mesenchymal stem cells.[28,29]

3.3. Time-Dependent Evolvement of F-actin Distribution and Vinculin Pattern. Cell adhesion process always involves cytoskeleton remodeling and focal adhesion formation.[3] The non-blocked PEF undergoes a process of actin filament reorganization after being seeded onto fibronectin-coated surface during 4 h of culture (Figure 2G−L). At 30 min, actin filaments are distributed throughout the nearly round cell body. The appearance of actin filament bundles (stress fibers) suggests the formation of focal adhesion in the cell cortex (Figure 2G). After another 30 min of culture, sparser and thicker actin filament bundles are localized in the edge of the cell in polygonal shape (Figure 2H). However,

(28) Lee, J. W.; Kim, Y. H.; Park, K. D.; Jee, K. S.; Shin, J. W.; Hahn, S. B. *Biomaterials* **2004**, *25*, 1901–1909.
(29) Siebers, M. C.; Walboomers, X. F.; van den Dolder, J.; Leeuwenburgh, S. C. G.; Wolke, J. G. C.; Jansen, J. A. *J. Mater. Sci.: Mater. Med.* **2008**, *19*, 861–868.

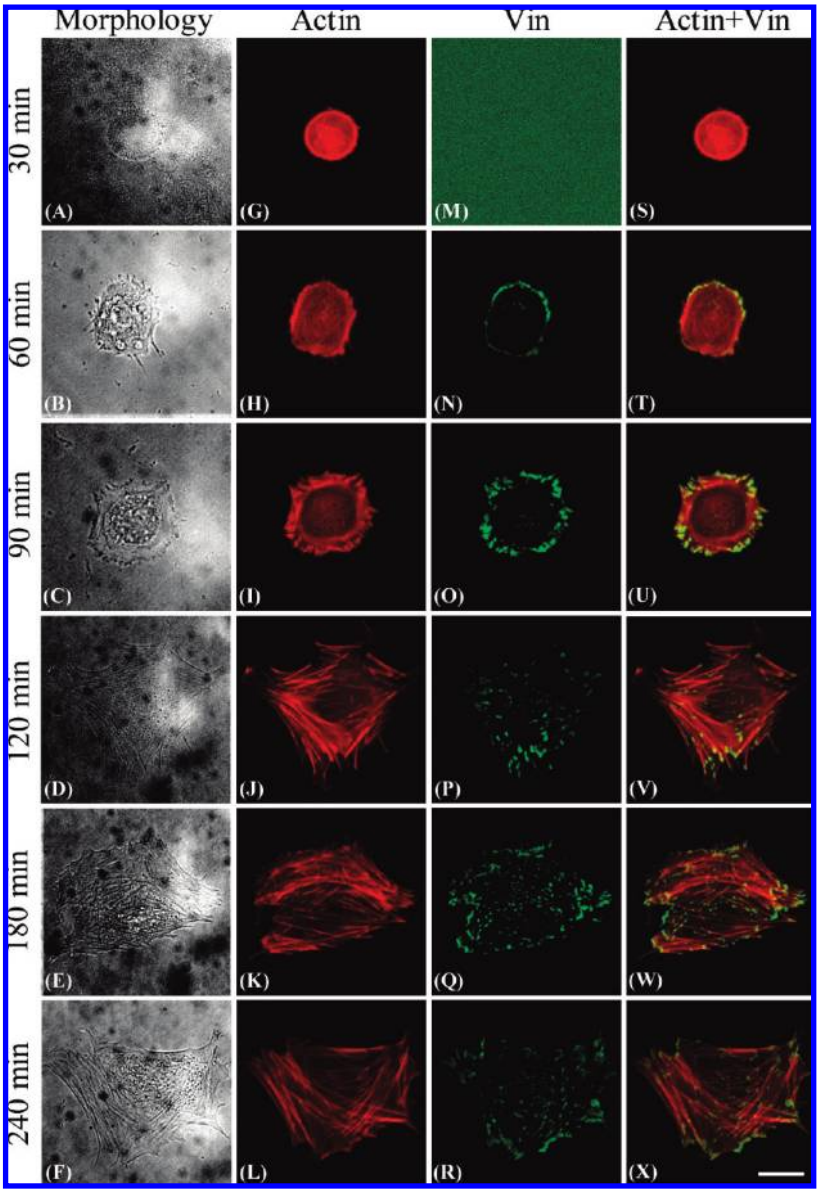

Figure 3. Time course study of cell morpholgy, F-actin distribution, and vinculin pattern of β_1-blocked PEFs. (A)−(F), phase contrast images; (G)−(L), fluorescence images of F-actin; (M)−(R), fluorescence images of vinculin; (S)−(X), merged images of F-actin and vinculin. Vin = vinculin. Bar, 20 μm.

actin filaments are still found in the cytoplasm. From 90 min onward, actin filament bundles become more prominent in the cellular periphery (Figure 2I−L). After 240 min of incubation, stress fibers are aligned to the edges of the cell in a highly ordered manner (Figure 2L). The appearance of stress fibers, as a result of cytoskeleton remodeling, is coupled with the formation of focal adhesion.[6] As shown in Figure 2M, focal adhesion lay at the cell periphery at 30 min where stress fibers exist. The corresponding merged image of actin and vinculin confirmed the colocalization of actin and vinculin near the cellular cortex (Figure 2S). After 60 min of culture, disparate and big focal adhesion plaques were found near the cell cortex. There are few focal adhesion plaques in the central portion of the cell at both 30 and 60 min. This phenomenon is consistent with the absence of stress fiber in central portion of cell body. From 90 min onward, the vinculin pattern becomes different. In Figure 2O, it is found that vinculin is scattered all over the cell body although focal adhesion plaques in the cell periphery appear larger than those in other regions. Similar focal adhesion pattern to that at 90 min is displayed after 120 min of culture (Figure 2P−R). At 240 min, focal adhesion is clearly spotted at the end of stress fibers (Figure 2X), confirming the colocalization of stress fiber and vinculin.

Blocking β_1 may affect actin filament remodeling and focal adhesion formation besides morphological evolution. At 30 min after cell seeding, actin filaments are present throughout the cytoplasm of the β_1-blocked PEF with round contour (Figure 3G). At the same time, vinculin is not observed in the TIRFM image as green background of the TIRFM image means no captured signals (Figure 3M). After another 30 min of culture, actin filaments still exist all over the cell body, and vinculin becomes visible in the cell periphery and particular regions of the cell body (Figure 3, panels H and N). The actin−riched lamellipodia in the cell membrane forms at 90 min after cell plating (Figure 3O). Vinculin is mainly colocalized with actin filament bundles at the cell edge (Figure 3U). After being cultured for more than 120 min, stress fibers are aligned parallel to the edge of the cell (Figure 3J−L) and vinculin were dispersed throughout the cell body (Figure 3P−R).

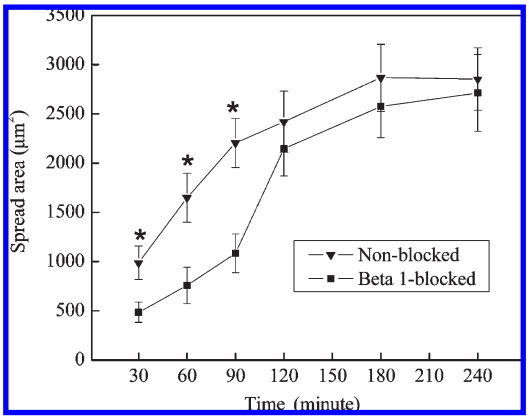

Figure 4. Spread area against time for non-blocked and β_1-blocked PEFs on fibronectin-coated surface within 4 h after cell seeding. $n = 80-100$ for each data point. *Significant difference from the corresponding value in β_1-blocked PEFs at the same time point ($p < 0.05$).

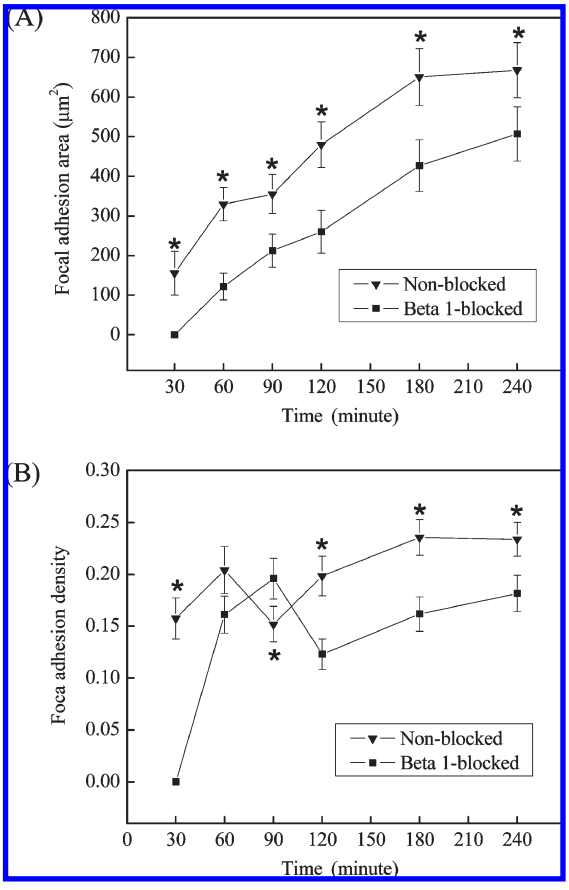

Figure 5. Focal adhesion area (A) and focal adhesion density (B) against time for non-blocked and β_1-blocked PEFs on fibronectin-coated surface within 4 h after cell seeding. $n = 80-100$ for each data point. *: Significant difference from the corresponding value in β_1-blocked PEFs at the same time point ($p < 0.05$).

Comparing the evolution of the F-actin distribution and the focal adhesion pattern in the non-blocked and β_1-blocked cells, the biggest difference is the lag time for initiating focal adhesion. For non-blocked cells, a lag time of around 30 min is needed for initiating focal adhesion formation. However, blocking β_1 integrin delays the focal adhesion formation, leading to an increase of lag time to 60 min, reflecting the dependence of activation of focal adhesion on β_1 integrin.

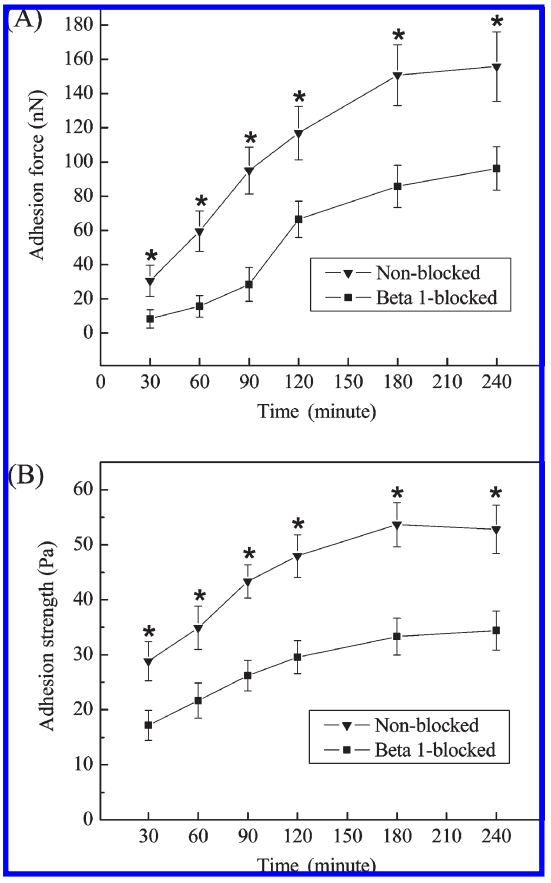

Figure 6. Adhesion force (A) and adhesion strength (B) against time for non-blocked and β_1-blocked PEFs on a fibronectin-coated surface within 4 h after cell seeding. $n = 80-100$ for each data points. *: Significant difference from the corresponding value in β_1-blocked PEFs at the same time point ($p < 0.05$).

Focal adhesion area, the area occupied by vinculin for each cell, was acquired from TIRFM images. Correspondingly, focal adhesion density, defined as focal adhesion area per spread area, was derived from analyzing the TIRFM and phase contrast images. The effect of culture time on focal adhesion area and focal adhesion density of non-blocked and β_1-blocked PEFs on fibronectin-coated surface is shown in Figure 5. A time-dependent increase in focal adhesion area of non-blocked and β_1-blocked cells is observed (Figure 5A). During the ascending process, the focal adhesion area of non-blocked cells always exceeded that of β_1-blocked cells. At 240 min post seeding, the focal adhesion area of non-blocked cells is 667 μm^2, 59% higher than that of β_1-blocked cells. The time-dependent change in the focal adhesion density is shown in Figure 5B. No single downward/upward trends in focal adhesion density against time are found in either non-blocked or β_1-blocked cells. For non-blocked cells, their focal adhesion density increases initially but then declines after 60 min post seeding. From 90 min, it starts to ascend again until reaching a maximum value at 240 min. A similar trend is also observed in β_1-blocked cells. During the late culture period (120−240 min), focal adhesion density of non-blocked cells is persistently higher than that of β_1-blocked cells.

3.4. Time-Dependent Change of Adhesion Force and Strength. Typically, cell adhesion is a strengthening process.[5] The effect of culture time on adhesion force is presented in Figure 6A. Adhesion force of non-blocked cells keeps on rising against time until stabilizes after 180 min. Similarly, the adhesion

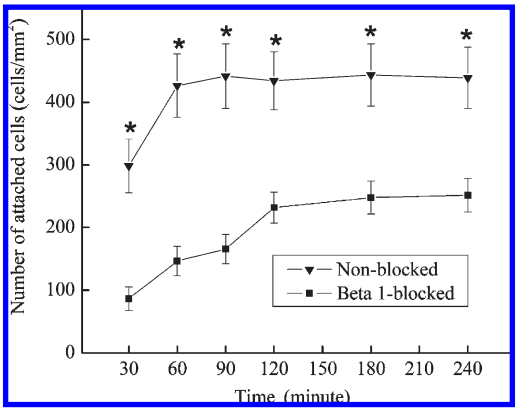

Figure 7. Number of attached cells against time for non-blocked and β_1-blocked PEFs on fibronectin-coated surface within 4 h after cell seeding. *: Significant difference from corresponding value in β_1-blocked PEFs at the same time point ($p < 0.05$).

force of β_1-blocked cells goes up with time. However, the adhesion force-time curve of non-blocked cells lies above that of β_1-blocked cells, indicating higher force is needed for the former to detach from the substrate following the same period of culture. Adhesion strength, defined as adhesion force per unit spread area, represents the maximum shear stress to detach cells. The effect of culture time on adhesion strength is shown in Figure 6B. As illustrated in Figure 6B, the adhesion strength maintains an upward trend over time during the 240 min of culture period. The maximum adhesion strength of non-blocked and β_1-blocked cells is 52.8 and 34.4 Pa, respectively. A similar tendency for the adhesion force to ascend with time was also noticed on chondrocytes by other researchers.[30,31]

3.5. Time-Dependent Change of Number of Attached Cells. To evaluate the affinity between cells and substrates, a cell attachment assay was carried out. On fibronectin-coated surface, both the number of attached non-blocked PEFs and the number of attached β_1-blocked PEFs exhibit an increase with culture time and reach a plateau (Figure 7). Comparatively, it is quicker for the number of attached non-blocked PEFs to reach its plateau. After 4 h of culture, the number of attached non-blocked cells is 43% less than that of β_1-blocked cells, implying that functional blocking of integrin β_1 significantly deteriorates the affinity of the integrin receptors for fibronectin ligands.

4. Discussion

Integrin-mediated cell adhesion is central to the physiological regulations of anchorage-dependent cells.[5] The initial integrin-ligand binding triggers cell spreading, integrin clustering, and focal adhesion, all of which contribute to the enhancement of adhesion force between cell and substrate.[9] Previous experimental data from other researchers unanimously demonstrated time-dependent increase in adhesion force for various types of cells on different substrate.[30−36] However, no result was reported on temporal fluctuation of adhesion force for β_1-blocked cells. It is demonstrated in our results that blocking the β_1 integrin subunit does not alter the ascending trend of adhesion force over time.

Cell spreading and focal adhesion formation contribute significantly to enhancement of cell adhesion.[9] There is a consensus on the fact that cells keep on spreading in the initial cell adhesion process.[27,30,33,37] To separate the effect of cell spreading and other factors, adhesion strength is defined to exclude the contribution of cell spreading to the adhesion strengthening process. As depicted in most published works, there is a trend of increase in adhesion strength over culture time.[30,33,34] In our results, the time-dependent increase of spread area and adhesion strength confirms that cell spreading alone cannot account for the increase of adhesion force during cell adhesion.

To explain the strengthening process during cell adhesion, many mechanical models have been proposed.[5,38,39] In these theoretical analyses, focal adhesion formation has been positively correlated with the enhancement of adhesion strength. At focal adhesion sites, the cell membrane stiffens and the binding strength intensifies because of the recruitment of focal adhesion protein and cytoskeleton remodeling.[38,40,41] For example, Ward et al. predicted that adhesion strength in the focal contact zone was 60%−650% higher than that in the non-focal contact zone.[38] In contrast, focal adhesion formation only resulted in 50%−200% of increase in adhesion strength through Gallant's simulation.[5]

Focal adhesion force (adhesion force at focal adhesion sites) is believed to be tightly connected with focal adhesion area. In Ward's model, focal adhesion force is nearly proportional to the focal adhesion density when the focal adhesion density is below a critical value.[38] Until now, there has been lack of experimental results about the quantitative relation between focal adhesion force and focal adhesion area because of the difficulty in the measurement of local adhesion force. However, the study of the association of traction force with focal adhesion provides some analogic results.[42,43] It is demonstrated in these works that traction force is almost linearly dependent on focal adhesion area, suggesting a possible linear relationship between focal adhesion force and focal adhesion area. If adhesion force within the non-focal adhesion zone is also proportional to the non-focal adhesion area, the linear relationship between adhesion strength and focal adhesion density may exist under particular conditions.

To check this hypothesis, adhesion strength-focal adhesion density curves for non-blocked and β_1-blocked PEFs were plotted in Figure 8. Beyond our initial expectation, six data points did not display a linear trend in Figure 8A,B. Nevertheless, the four data points at 90, 120, 180, and 240 min are linearly correlated in Figure 8A. Similarly, the three data points at

(30) Yamamoto, K.; Tomita, N.; Fukuda, Y.; Suzuki, S.; Igarashi, N.; Suguro, T.; Tamada, Y. *Biomaterials* **2007**, *28*, 1838–1846.
(31) Lee, M. C.; Sung, K. L. P.; Kurtis, M. S.; Akeson, W. H.; Sah, R. L. *Clin. Orthop.* **2000**, 286–294.
(32) Qin, T. W.; Yang, Z. M.; Wu, Z. Z.; Xie, H. Q.; Qin, H.; Cai, S. X. *Biomaterials* **2005**, *26*, 6635–6642.
(33) Huang, W.; Anvari, B.; Torres, J. H.; LeBaron, R. G.; Athanasiou, K. A. *J. Orthop. Res.* **2003**, *21*, 88–95.
(34) Yang, L.; Tsai, C. M. H.; Hsieh, A. H.; Lin, V. S.; Akeson, W. H.; Sung, K. L. P. *J. Orthop. Res.* **1999**, *17*, 755–762.
(35) Schinagl, R. M.; Kurtis, M. S.; Ellis, K. D.; Chien, S.; Sah, R. L. *J. Orthop. Res.* **1999**, *17*, 121–129.
(36) Rezania, A.; Healy, K. E. *J. Orthop. Res.* **1999**, *17*, 615–623.
(37) Cai, N.; Gong, Y. X.; Chian, K. S.; Chan, V.; Liao, K. *Biomed. Mater.* **2008**, *3*, 015014.
(38) Ward, M. D.; Hammer, D. A. *Biophys. J.* **1993**, *64*, 936–959.
(39) Ra, H. J.; Picart, C.; Feng, H. S.; Sweeney, H. L.; Discher, D. E. *J. Cell Sci.* **1999**, *112*, 1425–1436.
(40) Glogauer, M.; Arora, P.; Yao, G.; Sokholov, I.; Ferrier, J.; McCulloch, C. A. G. *J. Cell Sci.* **1997**, *110*, 11–21.
(41) Martinez, E. J. P.; Lanir, Y.; Einav, S. *Biomech. Model. Mechanobiol.* **2004**, *2*, 157–167.
(42) Balaban, N. Q.; Schwarz, U. S.; Riveline, D.; Goichberg, P.; Tzur, G.; Sabanay, I.; Mahalu, D.; Safran, S.; Bershadsky, A.; Addadi, L.; Geiger, B. *Nat. Cell Biol.* **2001**, *3*, 466–472.
(43) Tan, J. L.; Tien, J.; Pirone, D. M.; Gray, D. S.; Bhadriraju, K.; Chen, C. S. *Proc. Natl. Acad. Sci. U. S. A.* **2003**, *100*, 1484–1489.

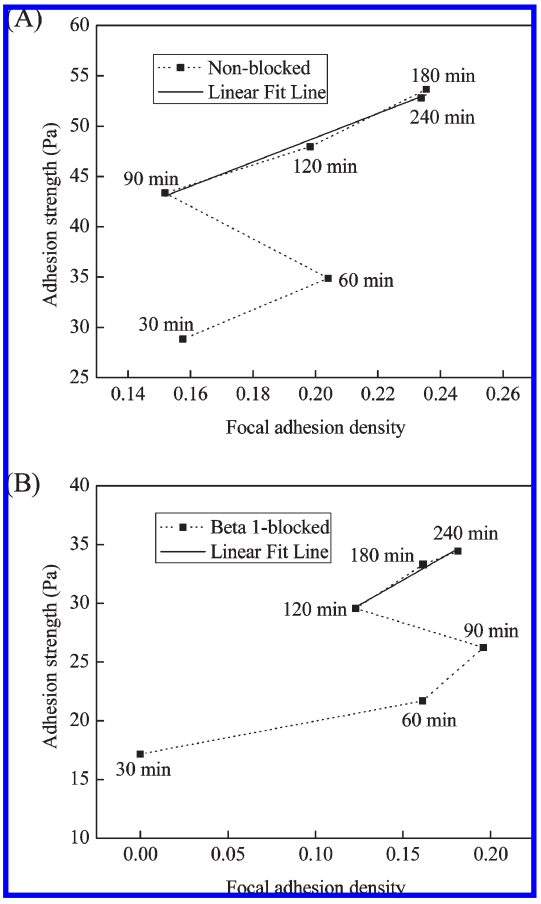

Figure 8. Relationship between adhesion strength and focal adhesion density. (A) Non-blocked PEFs on fibronectin-coated surface; $R^2 = 0.98$ for the linear fit. (B) β_1-blocked PEFs on fibronectin-coated surface; $R^2 = 0.97$ for the linear fit.

120, 180, and 240 min appear to lie roughly on a straight line in Figure 8B. Regression of the four data points in Figure 8A and the three data points in Figure 8B was carried out using the following function

$$\tau = \tau_{FA} \cdot P_{FA} + \tau_{NFA}(1 - P_{FA}) \quad (1)$$

where τ, τ_{FA}, τ_{NFA}, and P_{FA} are adhesion strength (or overall adhesion strength), focal adhesion strength, non-focal adhesion strength, and focal adhesion density, respectively. The slope and intercept of the fitted line correspond to $\tau_{FA} - \tau_{NFA}$ and τ_{NFA}, respectively. The focal adhesion and non-focal adhesion strength of non-blocked and β_1-blocked PEFs obtained by linear fitting are listed in Table 1.

The variation of adhesion strength of the two types of cells with respect to focal adhesion density during the cell adhesion process follows a similar trend. For instance, as shown in Figure 8A, adhesion strength of non-blocked cells increases with focal adhesion density from 30 to 60 min. After 60 min, the trend is reversed. The increase of focal adhesion density does not elevate the measured adhesion strength from 60 to 90 min. However, adhesion strength returns back to the escalating trend from 90 min onward. During 240 min of culture, increase of focal adhesion density does not inevitably bring about the ascent of adhesion strength. To explain this phenomenon, the peeling model and fracture model of cell detachment proposed by Ward et al. was tentatively used for reference 38. According to the distribution of focal adhesion within the cell boundary, adherent cells examined

Table 1. Focal Adhesion Strength (τ_{FA}) and Non-Focal Adhesion Strength (τ_{NFA}) of Non-Blocked and β_1-Blocked PEFs on Fibronectin-Coated Surface

cell type	τ_{NFA} (Pa)	τ_{FA} (Pa)
non-blocked PEFs	24.7	145.3
β_1-blocked PEFs	19.2	104.5

in our experiments were classified into two groups. The first group are cells whose focal adhesions are extremely concentrated on the cell periphery. The second group are cells with relatively uniform distribution of focal adhesion. After examining vinculin patterns in Figures 2 and 3, non-blocked PEFs at 30 and 60 min, and β_1-blocked PEFs at 60 and 90 min were classified the first group according to this criterion. Other cells except β_1-blocked PEFs at 30 min without the formation of focal adhesion are included in the second group. For the first group of cells, the detachment of adherent cells is believed to start from a progressive breaking of bonds at the central part of the cells where binding strength is weaker and cell membrane is more flexible than cell periphery. Afterward, the simultaneous failure of the bonds at the cell periphery with a dense focal adhesion structure leads to separation of the whole cell body from the substrate. Therefore, the dominant factor to determine adhesion strength of the cells in the first group is focal adhesion density. In other words, the cellular portion with non-focal adhesion makes little contribution to the overall adhesion strength. For the second group of cells, the distribution of focal adhesion is relatively uniform in the cell adhesion patch. Because of the stiffening effect of uniformly distributed focal adhesion on the cell membrane, the whole contact portion of the cells can be considered as a totally rigid entity approximately. Thus, the adherent part of the cell membrane with/without focal adhesion acts collectively to withstand the shear force applied by the micropipet. Under this condition, the adherent portion of the cell membrane without focal adhesions also made a definite contribution to the overall adhesion strength.

During the adhesion process of non-blocked cells, focal adhesion sites are mainly localized to cell periphery at 30 and 60 min. Cell detachment goes in the peeling mode. Adhesion strength ascends with an increase in focal adhesion density during this culture period. At or after 90 min, focal adhesions become uniformly dispersed in the cytoplasm of the cells. Cell detachment proceeds in fracture mode. Non-focal adhesion portion of membrane starts to make its contribution to the overall adhesion strength. That may explain the rise of adhesion strength under the circumstance that focal adhesion density declines from 60 and 90 min. After 90 min, focal adhesion is still dispersed throughout the spread portion of the cell membrane. As a result, adhesion strength increases in an approximate linear relationship over focal adhesion density. The variation of adhesion strength with focal adhesion density in β_1-blocked PEFs during 240 min of culture can be interpreted in a similar way.

The linear fit of adhesion strength with respect to focal adhesion density produces some useful information to comprehend cell adhesion. As shown in Table 1, focal adhesion strength is significantly higher than non-focal adhesion strength regardless to the type of cells used herein. The ratio of focal adhesion strength to non-focal adhesion strength in non-blocked and β_1-blocked PEFs is 5.9 and 5.4, respectively. These values just fall within the range predicted by Ward et al.[38] As focal adhesion strength, non-focal adhesion strength, and focal adhesion density are known, the contribution rate of focal adhesion to the overall adhesion strength can be derived. At 240 min, the contribution of focal adhesion to the overall adhesion strength is 64% in

non-blocked cells and 55% in β_1-blocked cells. Gallant et al. employed the siRNA technique to knockdown vinculin expression to investigate the importance of focal adhesion to adhesion strength.[9] In their results, focal adhesion makes up around 30% of the overall adhesion strength of NIH 3T3 fibroblasts. As shown in our results, a slight variation of focal adhesion density may induce a big change in adhesion strength because of the high ratio of focal adhesion strength to non-focal adhesion strength. In Gallant's report, very few vinculin plaques are found in NIH 3T3 fibroblasts compared to the higher focal adhesion density in PEFs. Therefore the increased contribution of focal adhesion to the overall adhesion strength is found in our results herein.

Functional blocking of β_1 integrin subunit was believed to impair the binding between integrin receptor and immobilized fibronectin and to reduce adhesion strength.[44,45] It is demonstrated in our results that non-blocked PEFs always possesses higher adhesion strength than β_1-blocked PEFs during 4 h of culture. Diminishment of adhesion strength by functional blocking of β_1 integrin was also confirmed indirectly on the adhesion of chondrocytes to cartilage tissue through flow cytometry by Kurtis et al.[46,47] In addition, it is found in our results that functional blocking of β_1 integrin reduces focal adhesion density, suggesting a downregulation of the vinculin expression which may be attributed to the impairment of fibronectin-integrin interaction. It was reported that targeted ablation or functional blocking of β_1 integrin results in a decrease of FAK expression level.[48,49] Thus, it is not surprising that functional blocking of β_1 integrin leads to a decrease of focal adhesion density. Furthermore, there is smaller focal adhesion strength and non-focal adhesion strength in β_1-blocked PEFs than in non-blocked PEFs as listed in Table 1. Therefore, it is the collective effect of smaller local adhesion strength (focal adhesion strength and non-focal adhesion strength) and of lower focal adhesion density that accounts for the weaker adhesion strength in β_1-blocked PEFs on a fibronectin-coated surface.

5. Conclusions

In this study, monoclonal antibodies were applied to block the β_1 integrin subunit in PEFs. The temporal effect of functional blocking of β_1 integrin on mechanotransduction of the cell was investigated with the TIRFM and micropipet aspiration technique. It is shown in our results that spread area, adhesion force, and adhesion strength of non-blocked and β_1-blocked PEFs on fibronectin-coated surface tend to increase over time during 4 h of cell seeding. Each mechanotransduction parameter of β_1-blocked cells is always smaller than those of non-blocked cells. Interestingly, there is tight relationship between adhesion strength and focal adhesion density in PEFs that can be explained by the peeling and fracture models. During the late culture period, adhesion strength increases linearly with focal adhesion density. On the basis of the fracture model, averaged focal adhesion strength and non-focal adhesion strength were deduced. Smaller adhesion strength is possessed by β_1-blocked PEFs than by non-blocked cells, which is attributed to lower focal and non-focal adhesion strength, as well as decreased focal adhesion density because of the blocking of β_1 integrin.

Acknowledgment. The authors acknowledge partial support of this project by the Singapore-University of Washington Alliance. Yang Tianyi is acknowledged for his helpful discussion.

(44) Kuo, S. C.; Lauffenburger, D. A. *Biophys. J.* **1993**, *65*, 2191–2200.
(45) Xiao, Y.; Truskey, G. A. *Biophys. J.* **1996**, *71*, 2869–2884.
(46) Kurtis, M. S.; Schmidt, T. A.; Bugbee, W. D.; Loeser, R. F.; Sah, R. L. *Arthritis Rheum.* **2003**, *48*, 110–118.
(47) Kurtis, M. S.; Tu, B. P.; Gaya, O. A.; Mollenhauer, J.; Knudson, W.; Loeser, R. F.; Knudson, C. B.; Sah, R. L. *J. Orthop. Res.* **2001**, *19*, 1122–1130.
(48) Bernard-Trifilo, J. A.; Kramar, E. A.; Torp, R.; Lin, C. Y.; Pineda, E. A.; Lynch, G.; Gall, C. M. *J. Neurochem.* **2005**, *93*, 834–849.
(49) Li, N.; Zhang, Y.; Naylor, M. J.; Schatzmann, F.; Maurer, F.; Wintermantel, T.; Schuetz, G.; Mueller, U.; Streuli, C. H.; Hynes, N. E. *EMBO J.* **2005**, *24*, 1942–1953.